Pergamon

Electrochimica Acta, Vol 39, No 3, pp 401–406, 1994

0013-4686/94 $6 00 + 0 00

A COMPUTER SIMULATION OF VOLTAMMOGRAMS DESCRIBING THE ACTIVE–PASSIVE TRANSITION OF Pb IN SULPHURIC ACID

F E VARELA, J R VILCHE and A J ARVIA

Instituto de Investigaciones Fisicoquímicas Teóricas y Aplicades (INIFTA),
Facultad de Ciencias Exactas, Universidad Nacional de La Plata, Sucursal 4, Casilla de Correo 16,
(1900) La Plata, Argentina

(*Received* 24 *May* 1993, *in revised form* 23 *August* 1993)

Abstract—A computer simulation of active–passive transition voltammograms of Pb in 5 M H_2SO_4 is presented The model implies alternative pathways leading to the formation of inner and outer structurally different $PbSO_4$ layers The inner layer consists of a disordered crystalline conducting phase, which is formed following an instantaneous nucleation and two-dimensional growth mechanism under charge-transfer control Electrodissolution of Pb proceeds by the diffusion of cations through the inner layer and, when Pb^{2+} ion concentration in solution exceeds the critical supersaturation concentration, the precipitation of the outer highly crystalline $PbSO_4$ layer takes place, leading to passivation Calculations are based on previously reported kinetic data Good agreement was found between theory and practice

Key words lead/sulphuric acid system, computer simulation of voltammograms, lead passivation, active–passive transitional modeling.

INTRODUCTION

Lead electrode reactions in aqueous sulphuric acid have been extensively studied using different stationary and transient techniques[1–3], although electrochemical processes leading to $PbSO_4$ formation on Pb are still open to discussion Several explanations about various stages participating in the overall reaction, and a dissolution–precipitation[3] or a solid-state mechanism[4, 5] have been advanced to interpret kinetic data Mechanisms combining both interpretations were also considered[6, 7]

Recently[8] it was shown that the active–passive transition of Pb in aqueous H_2SO_4 can be described by a complex reaction model involving the nucleation and growth of solid $PbSO_4$, this process occurring in parallel with Pb electrodissolution and $PbSO_4$ precipitation Evidence for this mechanism came out from ring-disk electrode data Dissolved Pb^{2+} ions from a Pb disk could be detected through this technique and it was noted that the ring current was always much smaller than the value calculated from the collection efficiency This difference was interpreted through the simultaneous $PbSO_4$ surface layer growth and Pb electrodissolution, the surface film playing a key role in the kinetics of the overall reaction The mechanism implies the formation of a thin ionically conducting barrier[8], which assists the migration of Pb^{2+} ions This explanation was firstly advanced by Pavlov[9] and Pavlov and Popova[10] who admitted that at positive potentials, the inner part of the $PbSO_4$ layer acted simultaneously as a perm-selective membrane for Pb^{2+} ions, and as a blocking membrane for the access of SO_4^{2-} ions to the interfacial regions

This work describes a computer simulation of experimental single linear sweep voltammograms based upon the model previously used to interpret the potentiostatic transients of $PbSO_4$ electroformation on Pb electrodes Calculations are based on the following assumptions (i) The single linear potential swep is the sum of an infinite number of potential steps ΔE, (ii) the duration of each step is Δt, so that $\Delta E/\Delta t = v$, where v is the potential sweep rate, (iii) the electrode surface coverage at each $E + \Delta E$ value remains constant The potential dependence of kinetic data derived from potentiostatic experiments previously reported[8] is used A good agreement between simulation and experimental results is accomplished

EXPERIMENTAL

The experimental setup was the same as already described elsewhere[8, 11, 12] "Specpure" lead discs (Johnson Matthey Chemicals Ltd, 0 30 cm^2 apparent area) embedded in PTFE holders were used as working electrodes These electrodes were mechanically polished with 600 and 1200 grade emery papers and thoroughly rinsed in triply-distilled water Electrochemical runs were performed in aqueous 5 M H_2SO_4 at 25°C, under purified nitrogen gas saturation The solution was prepared from analytical grade (p a Merck) reagent and Milli-Q* water Potentials were measured, and referred to in the text, against a $Hg/Hg_2SO_4/K_2SO_4$(sat) electrode, $E^0_{Hg/Hg_2SO_4} = 0\,68$ V (vs *she*)

Prior to each run the working electrode was cathodized at $-1\,3$ V for $\tau_0 = 5$ min, *ie* in the hydrogen evolution reaction (*her*) potential range, to achieve a reproducible electroreduced Pb surface Subsequently, the electrode was subjected to linear potential sweep cycling between cathodic ($E_{s,c}$) and anodic ($E_{s,a}$) switching potentials in the $0\,002 \leqslant v \leqslant 0\,200\ V\,s^{-1}$ range

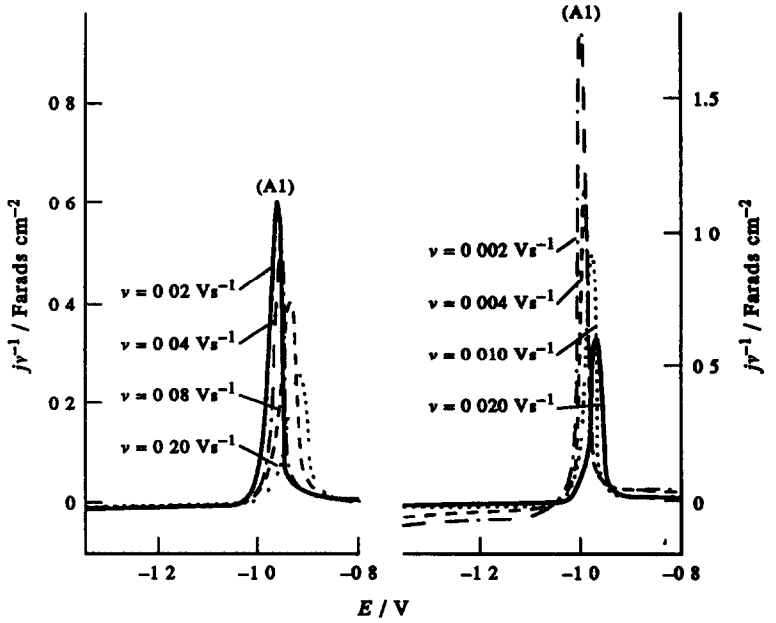

Fig 1 Experimental voltammetric data depicted as jv^{-1} vs E plots, 5 M H_2SO_4, 25°C Influence of v

Computer programs in QUICK-BASIC 4 5 were run on an IBM PS/2 50 computer

RESULTS

Positive potential going single sweep voltammograms of Pb in aqueous 5 M H_2SO_4 run from $E_{s,c} = -1\,350$ V to $E_{s,a} = -0\,800$ V within the $0\,002 \leqslant v \leqslant 0\,200$ V s^{-1} range, are shown in Fig 1 as jv^{-1} vs E plots The potential scan exhibits a well-defined anodic current peak (A1) corresponding to the electro-oxidation of Pb to Pb(II) followed by a wide passive current region[11] The initiation of peak A1 is close to the reversible potential of the Pb/$PbSO_4$ electrode, $E_{Pb/PbSO_4/5\,M\,H_2SO_4}$/V (vs *Hgse*) = −1 036, at 25°C[13] Cyclic voltammograms of Pb in aqueous 5 M H_2SO_4 have been previously described[8, 11] The jv^{-1} vs E plots show that as v decreases, $j_{p,A1}$, the height of peak A1, increases and $E_{p,A1}$, the peak potential shifts negatively The sharpness of peak A1 defined as the peak height to peak width ratio at one half peak height decreases with v

INTERPRETATION AND DISCUSSION

1 *The reaction pathway*

The equation describing the anodic current behaviour during the active–passive transition at the Pb/$PbSO_4$/H_2SO_4 interface, as discussed in a previous work[8], consists of the sum of three separate contributions

$$j(t) = j_g(t) + j_d(t) + j_f(t) \quad (1)$$

where $j_g(t)$, $j_d(t)$ and $j_f(t)$ stand for the apparent current density contribution due to instantaneous nucleation and growth of a $PbSO_4$ conducting film, Pb electrodissolution from the $PbSO_4$-film-free Pb surface, and Pb electrodissolution through the $PbSO_4$-covered Pb surface, respectively

The growth of the inner $PbSO_4$ conducting film fits an instantaneous nucleation and two dimensional growth under charge-transfer control kinetics[14], *ie*·

$$j_g(t) = P_1 t \exp(-P_2 t^2) = q_g \, d\theta'/dt, \quad (2)$$

where θ' is the fractional Pb surface coverage by the inner $PbSO_4$ layer (Fig 2), q_g is the apparent $PbSO_4$ layer charge density when $\theta' = 1$ and P_1 and P_2 are given by

$$P_1 = 2\pi n F M h N_0 k^2 \rho^{-1} \quad (3)$$

$$P_2 = \pi N_0 M^2 k^2 \rho^{-2}, \quad (4)$$

where N_0 is the number of nuclei instantaneously formed, k is the average film growth rate constant M, ρ and h are the molecular weight, the density and the average $PbSO_4$ layer height Since $\theta' \to 1$ when

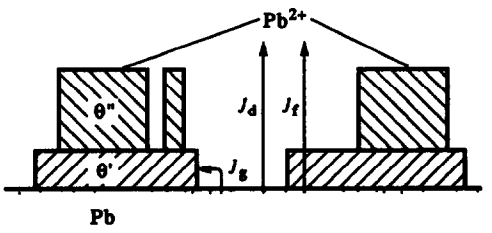

Fig 2 Scheme of the passivation process [ ] Pb, [///] $PbSO_4$ conducting layer (θ'), [\\\] $PbSO_4$ passivating layer (θ'') Different anodic current contributions are indicated

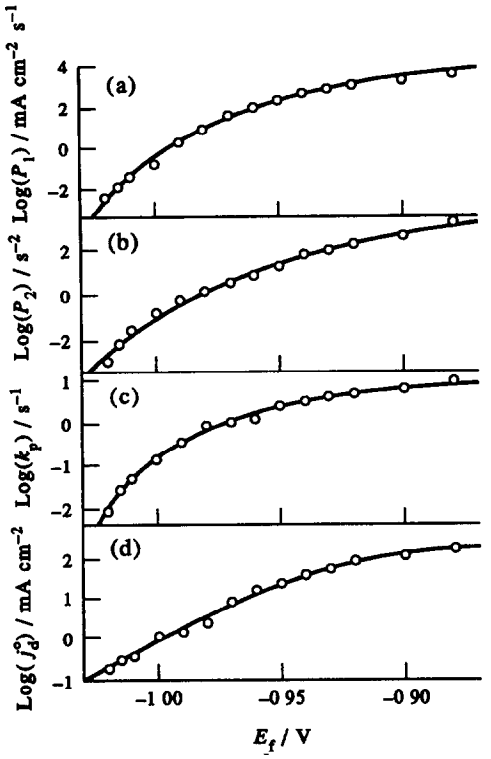

Fig 3 Dependence of model parameters on potential (a) P_1, (b) P_2, (c) k_p, and (d) j_d^0 Theoretical curves were drawn from equations (10)–(13) (full traces)

$t \rightarrow \infty$, from equation (2), it results that

$$q_g = P_1/2P_2 \tag{5}$$

and then, for $0 \leqslant t \leqslant \infty$

$$\theta' = 1 - \exp(-P_2 t^2) \tag{6}$$

The second term, $j_d(t)$, corresponds to Pb electrodissolution as Pb^{2+} ion in solution from bare lead Accordingly, $j_d(t)$ can be expressed as follows

$$j_d(t) = j_d^0(1 - \theta'), \tag{7}$$

where j_d^0 is the Pb electrodissolution current for $\theta' = 0$ ($t = 0$)

In equation (1) the term $j_f(t)$ corresponds to the transport of Pb^{2+} ions through the inner $PbSO_4$ film, and subsequent precipitation on top of this film leading to the outer passivating layer In this way,

$$j_f(t) = 2Fk_f(\theta' - \theta''), \tag{8}$$

where $\theta'' \leqslant \theta'$, θ'' being the fractional coverage by the outer $PbSO_4$ layer The rate equation of surface blockage due to the outer passivating layer (θ'') is given by the equation

$$d\theta''/dt = k_p(\theta' - \theta'') \tag{9}$$

On the basis of equations (1), (2), (7), (8) and (9), the experimental potentiostatic transients were reasonably reproduced with the set of potential dependent parameters shown in Fig 3, using non-linear fit routines

The potential dependence of the model parameters were obtained from previous experiments using potential step techniques As expected, the parameter potential dependence followed a linear logarithmic relationship[8], but a more accurate estimation of these parameters was achieved by using

$$\log P_1 = 31\,5\beta^2/(\beta^2 + 2\,5 \times 10^{-3}) - 26\,2 \tag{10}$$

$$\log P_2 = 49\,8\beta^2/(\beta^2 + 3\,9 \times 10^{-3}) - 44\,5 \tag{11}$$

$$\log k_p = 29\,5\beta^2/(\beta^2 + 6\,5 \times 10^{-4}) - 28\,2 \tag{12}$$

$$j_d^0 = 237\,4\left(\frac{0\,091\exp(38\,95\varepsilon)}{1 + 0\,091\exp(38\,95\varepsilon)}\right)^2, \tag{13}$$

with $\beta = E + 1\,13$ V and $\varepsilon = E + 0\,99$ V These functions are plotted in Fig 3 (full traces) along with experimental data (open circles) For the potential range of the simulation, $k_f = 7 \times 10^{-8}$ mol cm^{-2} s^{-1}

2 Simulation of anodic single potential sweep voltammograms

A diagram of the simulation procedure is illustrated in Fig 4 The transient at different potentials $n\Delta E$, $(n + 1)\Delta E$, $(n + 2)\Delta E$, and $(n + 3)\Delta E$ are shown Calculation starts at a certain coverage (see arrow in Fig 4) on the $n\Delta E$ transient, and θ' is allowed to grow for a time $(\Delta t)_n$, so that the current density j_n is computed along with the surface coverage θ'_n and θ''_n Subsequently, the potential is stepped to $(n + 1)\Delta E$, the parameters for this new potential are calculated for θ'_n and θ''_n and the simulation continued from $(t_i)_{n+1}$ to $(t_i + \Delta t)_{n+1}$ At the end of the new increment, the coverages θ'_{n+1} and θ''_{n+1} and the current density j_{n+1} are calculated The process is repeated until $\theta'' > 99\,99\%$ The resulting voltammogram is thus generated by displaying j_n vs $\Sigma\Delta E$ for $\Delta E \rightarrow 0$ It should be noted that, because of the

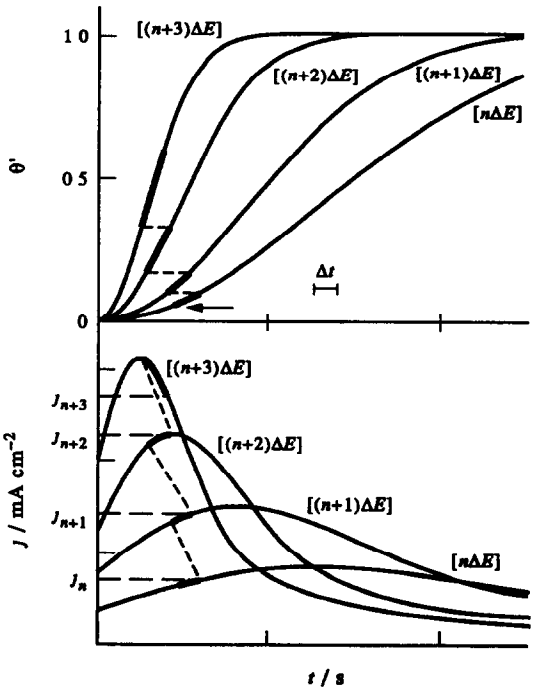

Fig 4 Computer simulation scheme

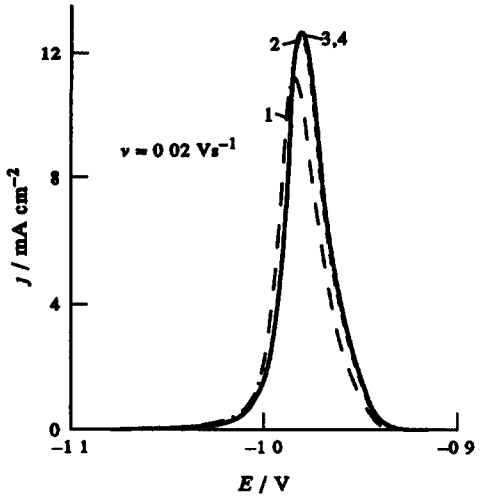

Fig 5 Simulated voltammogram for different ΔE values $\Delta E = 10$ mV, (- -) curve 1, $\Delta E = 1$ mV, (----) curve 2, $\Delta E = 0.1$ mV, ( ) curve 3, $\Delta E = 0.01$ mV, (——) curve 4

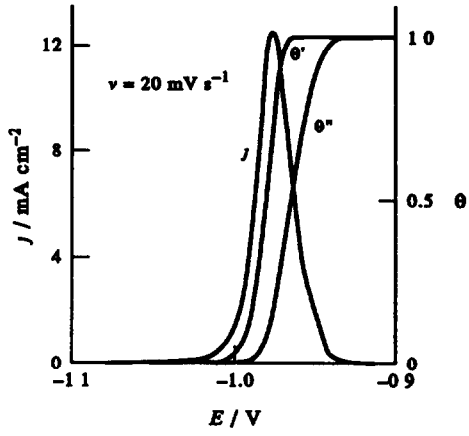

Fig 6 Typical simulated voltammogram and surface coverages for $v = 20$ mV s^{-1} Initial surface coverage $\theta'_0 = 0.5\%$, $\Delta E = 0.01$ mV

exponential dependence of the model parameters on potential[8], the calculation procedure requires the choice of an arbitrary initial surface coverage, otherwise the program will not converge for $\Delta E \to 0$ The influence of ΔE on the convergence for $\theta'_0 = 0.0005$ is illustrated in Fig 5 Throughout the present work the initial surface coverage was taken as 0.05% at $E_{s,c}$

A typical simulated voltammogram and the variation of θ' and θ'' on potential are shown in Fig 6 The agreement between results from the simulation and experimental data emerging from the comparisons of Fig 1 with Figs 6 and 7 is very good Note also that although $\theta' = 72\%$ at the current peak value, θ'' is lower than 20% This explains why the charge measured up $E_{p\,A1}$ is lower, approximately 45%, than the overall anodic charge involved in the electro-oxidation of Pb to $PbSO_4$[8]

3 *The influence of the potential sweep rate*

The influence of v in the simulation was investigated for 0.05% as initial surface coverage At constant v, as ΔE was diminished, convergence was as expected, and for convenience $\Delta E = 0.01$ mV was chosen The resulting voltammograms plotted as jv^{-1} vs E are shown in Fig 7, which exhibit identical trends as the experimental ones at least for $v \geqslant 0.01$ V s^{-1}

The model reproduces the dependence of $E_{p,A1}$ and $\log j_{p,A1}$ on $\log v$, Fig 8a and b, respectively[8] However, for $v < 0.01$ V s^{-1} the simulated values of $j_{p,A1}$, q_M, the anodic apparent charge density measured from $E_{s,c}$ up to $E_{p,A1}$, (Fig 9a), and q_a, the overall anodic apparent charge density (Fig 9b), are higher than the experimental ones These deviations can be explained by a difference between the threshold potential of Pb electrodissolution to Pb^{2+} and that of $PbSO_4$ nucleation This difference is not considered in the above described model As a matter of

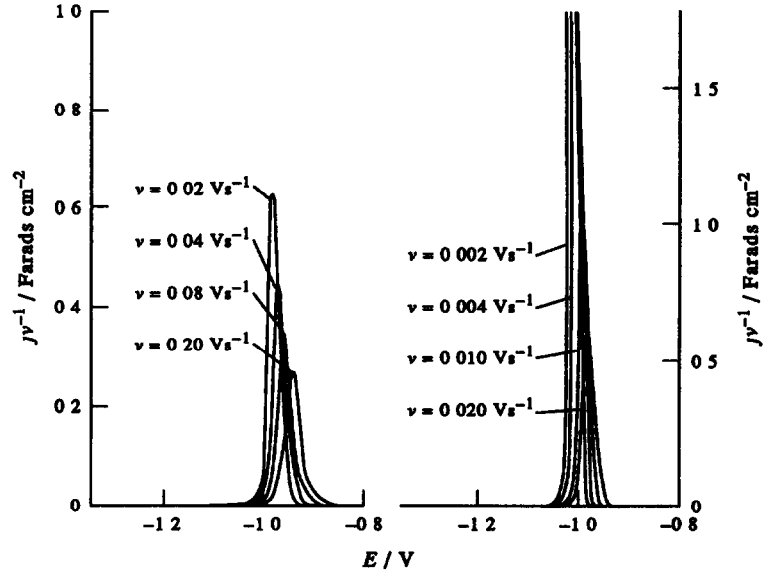

Fig 7 Simulated voltammetric data depicted as jv^{-1} vs E plots Influence of v

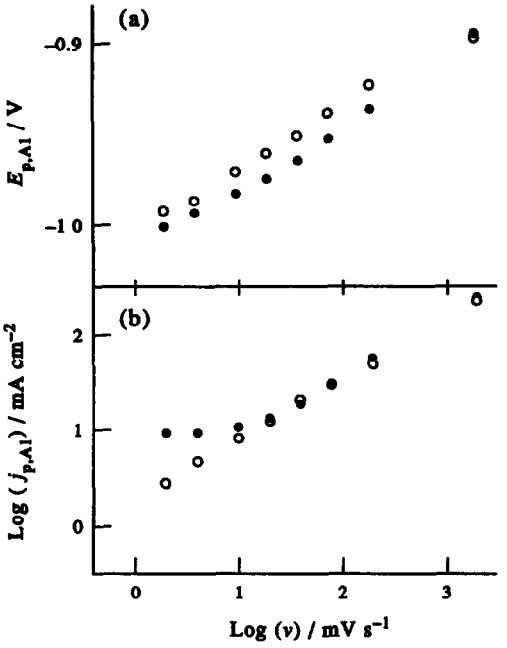

Fig. 8 Dependence of (a) $E_{p,A1}$, and (b) $j_{p\ A1}$ on v, (○) simulated and (●) experimental data obtained from voltammograms run between $E_{s,c} = -1.35$ V and $E_{s,a} = -0.80$ V in the $0.002 \leqslant v \leqslant 2.0$ V s^{-1} range, 5 M H_2SO_4, 25°C

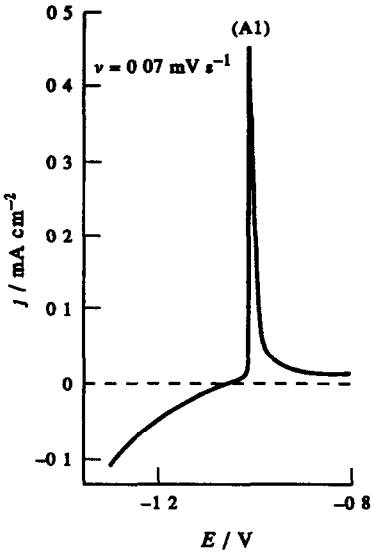

Fig 10 Voltammogram run at $v = 0.07$ mV s^{-1} between $E_{s,c} = -1.30$ V and $E_{s,a} = -0.80$ V, 5 M H_2SO_4, 25°C

fact, at a very low sweep rate, *ie* $v = 7 \times 10^{-5}$ V s^{-1} (Fig. 10), an anodic current appears *ca* 35 mV before $PbSO_4$ nucleation starts Accordingly, values of simulated currents and charges involved in the passivation process resulted higher than the experimental ones In this case the electrodissolution process is determined by the Pb^{2+} saturation concentration at the electrochemical interface which is *ca* $c_{Pb^{2+}} \cong 5.6 \times 10^{-6}$ mol dm^{-3} in 5 M sulphuric acid solution[15] As $c_{Pb^{2+}}$ is reached, $PbSO_4$ precipitation occurs without previous film formation by nucleation and growth from solid state Then, the question whether $PbSO_4$ film formation takes place through the direct precipitation of Pb^{2+} in solution leading to partial passivation and nucleation at free areas of the electrode surface, or through a solid state process beneath $PbSO_4$ is open for further investigation

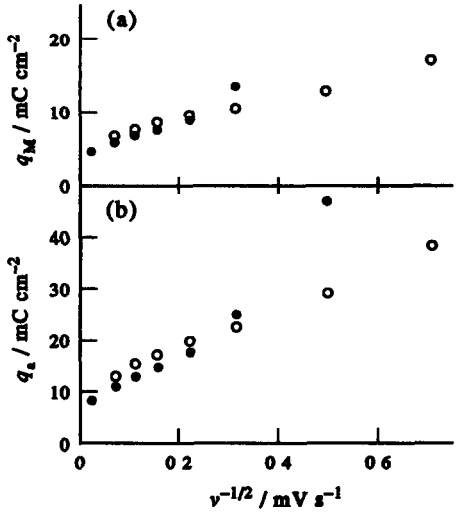

Fig 9 Dependence of (a) q_M and (b) q_s on $v^{-1/2}$, (○) simulated and (●) experimental data experimental data obtained from voltammograms run between $E_{s,c} = -1.35$ V and $E_{s,a} = -0.80$ V in the $0.002 \leqslant v \leqslant 2.0$ V s^{-1} range 5 M H_2SO_4, 25°C

CONCLUSIONS

A computer simulation of voltammograms describing the active–passive transition at the $Pb/PbSO_4/H_2SO_4$ interface is presented The model is based on a previous complex mechanistic interpretation based upon potentiostatic current transients

The reaction model implies the formation of a thin barrier film which behaves an an ionic conductor Pb^{+2} ions are transferred through this film, the concentration of Pb^{2+} aquated ions is increased, and highly crystalline $PbSO_4$ precipitate passivates the electrode

The voltammogram simulations procedure considers that a single linear potential sweep is the sum of an infinite number of potential increments, and that between successive increments the surface coverage of the electrode remains constant Good qualitative and quantitative agreements between theory and potentiodynamic experiment for $v \geqslant 0.1$ V s^{-1} are found

Acknowledgements—This research project was financially supported by the Consejo Nacional de Investigaciones Cientificas y Técnicas, the Comision de Investigaciones Cientificas de la Provincia de Buenos Aires and the Fundacion Antorchas

REFERENCES

1 T F Sharpe, in *Encyclopedia of Electrochemistry of the Elements* (Edited by A J Bard), Vol 1, pp 235–347 Marcel Dekker, New York (1973)

2 H Bode, *Lead–Acid Batteries*, John Wiley, New York (1977)
3 K R Bullock and D Pavlov (Editors), *Advances in Lead–Acid Batteries*, The Electrochemical Society, Pennington, New Jersey (1984)
4 G Archdale and J A Harrison, *J electroanal Chem* **34**, 21 (1972), **39**, 357 (1972)
5 N A Hampson and J B Lakeman, *J electroanal Chem* **107**, 177 (1980)
6 S B Hall and G A Wright, *Corros Sci* **31**, 709 (1990)
7 C V D'Alkaine and J M Cordeiro, in *Advances in Lead–Acid Batteries* (Edited by K R Bullock and D Pavlov), p 190 The Electrochemical Society, Pennington, New Jersey (1984)
8 F E Varela, M E Vela, J R Vilche and A J Arvia, *Electrochim Acta* **38**, 1513 (1993)
9 D Pavlov, *Electrochim Acta* **13**, 2051 (1968), **23**, 845 (1978)
10 D Pavlov and R Popova, *Electrochim Acta* **15**, 1483 (1970)
11 F E Varela, L M Gassa and J R Vilche, *Electrochim Acta* **37**, 1119 (1992)
12 F E Varela, L M Gassa and J R Vilche, *J electroanal Chem* **353**, 147 (1993)
13 Z Galus, in *Standard Potentials in Aqueous Solution* (Edited by A J Bard, R Parsons and J Jordan), pp 220–235 Marcel Dekker, New York (1985)
14 J A Harrison and H R Thirsk, in *Advances in Electroanalytical Chemistry* (Edited by A J Bard), Vol 5, pp 67–148 Marcel Dekker, New York (1971)
15 K Kanamura and Z Takehara, *J electrochem Soc* **139**, 345 (1992)